Trials in Vaccinology 4 (2015) e80–e87

Contents lists available at ScienceDirect

Trials in Vaccinology

journal homepage: www.elsevier.com/locate/trivac

Neem leaf glycoprotein optimizes effector and regulatory functions within tumor microenvironment to intervene therapeutically the growth of B16 melanoma in C57BL/6 mice

Subhasis Barik [a], Saptak Banerjee [a], Madhurima Sarkar [a], Avishek Bhuniya [a], Soumyabrata Roy [a], Anamika Bose [b], Rathindranath Baral [a,*]

[a] Department of Immunoregulation and Immunodiagnostics, Chittaranjan National Cancer Institute (CNCI), 37, S. P. Mukherjee Road, Kolkata 700026, India
[b] Department of Molecular Medicine, Bose Institute, C.I.T. Scheme, Kolkata, India

ARTICLE INFO

Article history:
Received 24 September 2013
Received in revised form 8 November 2013
Accepted 8 November 2013
Available online 6 December 2013

Keywords:
Cancer
Tumor microenvironment
Neem leaf glycoprotein

ABSTRACT

Therapy with neem leaf glycoprotein (NLGP) inhibits murine B16-melanoma *in vivo* and improves survivability. Studies on tumor-microenvironment (TME) from NLGP treated mice (NLGP-TME) suggests that anti-tumor effect is directly associated with enhanced $CD8^+$T cell activity, dominance of type 1 cytokines/chemokine network with downregulation of suppressive cellular functions. NLGP-TME educated $CD8^+$T cells showed higher perforin and granzymeB expression with greater *in vitro* cytotoxicity against B16 melanoma. These $CD8^+$T cells showed proportionally lower FasR expression, denotes prevention from activation induced cell death by NLGP. Accumulated evidences strongly suggest NLGP influenced normalized TME allows $CD8^+$T cells to perform optimally to inhibit melanoma growth.

Introduction

Melanomas are considerably more immunogenic than other tumors [1], but current immunotherapeutic approaches for melanoma patients have gained limited success [2]. Recent study identified tumor promoting effect of suppressor cells within melanoma tumor microenvironment (TME) [3]. Although, melanoma-specific $CD8^+$T-cell responses can often be generated in patients naturally or through vaccination [4], tumor grows consistently and suggests dampening of tumor-specific immune responses. Regulatory immune cells and suppressive cytokine milieu within TME negatively instruct effector T-cell functions. Accordingly, TME organized immunosuppressive network protects tumor cells from being attacked by immune effector cells [5] leading to tumor growth, metastasis and failure of immunotherapeutic modalities [6]. Thus, effector T-cell activation needs to be assisted by the normalization of TME.

Neem leaf preparation (NLP) is tested extensively in prophylactic settings on murine carcinoma, melanoma and sarcoma [7,8]. Neem leaf glycoprotein (NLGP), a nontoxic immunomodulatory principle of NLP, was examined *in vitro* [9] and in peripheral immune systems of tumor bearers [10–12], it activates effector cells, including T [9,13] and NK-cells [13], matures dysregulated dendritic cells [9], downregulates suppressor cells [14], polarizes type2 immune pattern into type1 by altering cytokine-chemokine signaling [15,16]. In this perspective, here, we wanted to examine the therapeutic role of NLGP on mouse melanoma and to understand the mechanism of alteration in tumor growth by analyzing TME. NLGP altered melanoma TME was specially tested for any noteworthy modulation in the functioning of $CD8^+$ cytotoxic T-cells that could be translated into maximum therapeutic benefits.

Materials and methods

Reagents and antibodies

Duelbeco's Modified Eagle's medium (DMEM) and fetal bovine serum (FBS) were purchased from Life Technologies (NY, USA). Magnetic Activated Cell Sorter (MACS) was procured from Miltenyi Biotech (GmbH, Germany). CD4-FITC/Cy-chrome, GR1-FITC mAbs were procured from BD Pharmingen (San Diego, CA, USA). CD25 (PE), CD69 (FITC) were purchased from Biolegend (USA) and cytokine neutralizing mAbs were obtained from e-Biosciences. Fluorescence- or peroxidase-labeled secondary antibodies were procured from e-Biosciences. CytoFix/CytoPerm solutions, IFNγ/IL-10 estimation kits, 3,3′,5,5′-tetramethylbenzidine sub-

* Corresponding author. Tel.: +91 033 24765101x334; fax: +91 033 24757606.
E-mail addresses: baralrathin@hotmail.com, rathindranath.baral@cnci.org.in (R. Baral).

http://dx.doi.org/10.1016/j.trivac.2013.11.001
1879-4378/

strate solutions were obtained from BD Pharmingen, USA. Cytotoxicity detection LDH release kit was procured from Roche Diagnostics (Mannham, Germany). Chemiluminescence detection kit was purchased from Pierce (Rockford, IL, USA). Tri-reagent for RNA isolation and RevertAid™ First Strand cDNA Synthesis Kit were procured from Invitrogen, Camarillo, CA, USA and Fermentas, K1622, USA, respectively. Reverse transcription-PCR primers were designed and procured from MWG-Biotech AG (Bangalore, India).

Neem leaf glycoprotein (NLGP)

Extract from neem *(Azadirachta indica)* leaves was prepared by the method as described [8,7]. Mature leaves of same size and color (indicative of same age), taken from a standard source were shed-dried and pulverized. Leaf powder was soaked overnight in phosphate buffered saline (PBS); pH 7.4, supernatant was collected by centrifugation at 1500 rpm. Neem leaf preparation (NLP) was then extensively dialyzed against PBS, pH 7.4 and concentrated by Centricon Membrane Filter (Millipore Corporation, Bedford, MA, USA) with 10 kDa molecular weight cut off. Glycoprotein present in this preparation (NLGP) was isolated and characterized by the method described [8,16]. NLGP is a purified glycoprotein which gives single band in native page, three different bands in SDS–PAGE having molecular weight of 47, 23 and 15 kDa. Its molecular weight is around 90 kDa. The purity of NLGP was checked by Size Exclusion-HPLC (SE-HPLC) in a protein PAK 300 SW column of 7.5 mm (ID) × 30 cm, as described [9]. Quantification NLGP is done by measuring its protein concentration [19].

Animals, tumor cells and NLGP treatment

Female C57BL6/J mice, 4–6 weeks of age with average body weight of 25 g were obtained from Institutional Animal Facilities, CNCI, Kolkata, India. Autoclaved dry pellet diet (Epic Laboratory Animal Feed, Kalyani, India) and water were given *ad libitum*. Animal experiments were performed according to the guidelines established by the Institutional Animal Care and Ethics Committee of CNCI, Kolkata, India and this committee approved the present study. Solid melanoma tumors were developed in mice by inoculation of 2×10^5 B16 Melanoma F10 cells (maintained in DMEM) subcutaneously into syngenic mice and allowed to grow as solid tumor. Tumors were removed from diseased mice and used in under mentioned experiments.

NLGP was administered subcutaneously in the left flange to female C57BL6/J mice at 25 μg/mice dose weekly for 4 weeks in total in the experimental group.

Tumor microenvironment

Tumor tissues were harvested from experimental animals and weighed. The identical weight of tumor tissues from NLGP and PBS mice was minced and exposed to repetitive freeze-thaw cycles as described [17,18]. Prepared lysates were centrifuged at 10,000 rpm for 10 mins and supernatant was collected to use as TME. TME from either PBS or NLGP treated mice was designated as PBS-TME and NLGP-TME respectively. These TMEs were used for *in vitro* treatment and estimation of soluble cytokines and growth factors. For western blot analysis after repetitive freeze-thaw cycles tumors were dissolved in RIPA buffer and kept at 4°C for 30 mins and supernatants were collected by centrifugation. Protein concentration was measured by Lowry's method using Folin-phenol reagent [19].

Cytokine detection assay

To quantify cytokines, solid tumors harvested at different days after tumor inoculation and TME was prepared as mentioned above. Secretion of different cytokines (IFNγ, IL-12p70, IL-10, IL-6, IL-2 and TGFβ) within TME was assessed by ELISA and optical density was measured at 450 nm using microplate reader (BioTek Instruments Inc., Vermont, USA).

TME educated effector cells

Splenic mononuclear cells ($1X10^6$ cells) from normal mice, were purified by density gradient centrifugation on Lymphocyte separating solution (LSM) and exposed to either PBS-TME or NLGP-TME (10 μg of protein) for 120 hrs at 37 °C on anti-CD3 antibody coated plate with supply of 5% CO_2. After incubation, non-adherent fractions were collected as effector cells. $CD8^+$T-cells were purified from effector cell population using magnetic assisted cell sorting (MACS).

Purification of $CD8^+$T-cells, regulatory T cells (Tregs) and myeloid derived suppressor cells (MDSCs) from solid melanoma by MACS

$CD8^+$, $CD4^+CD25^+$ and $GR1^+$ cells were purified by MACS. In brief, after harvesting tumor from tumor-bearing mice, tumor tissues were minced and treated with collagenase (1 mg/ml) and hyanuronidase (1 mg/ml) for 10 mins. Digested tissues then passed through a cell strainer (BD BioSciences, USA) to get single cells. Single cells were labeled with cocktail of antibodies, conjugated with magnetic beads and passed through a magnetic column. Purity of cells was checked by flow cytometry by labeling with appropriate antibodies.

Functional assays for T cells

RBC depleted splenic mononuclear cells (1×10^6 cells) were incubated with either PBS-TME or NLGP-TME for 120 hrs at 37 °C with supply of 5% CO_2. Following co-incubation non-adherent fractions were collected as effector cells and $CD8^+$T-cells were purified from this cellular population by MACS. TME exposed $CD8^+$T cells

Table 1
Primer sequences of various cytokine genes studied.

Name	Primer sequences (5′-3′)	Product size
β-Actin-forward	CAACCGTGAAAAGATGACCC	228 bp
β-Actin-reverse	ATGAGGTAGTCTGTCAGGTC	
IFNg-forward	ACTGGCAAAAGGATGGTGAC	237 bp
IFNg-reverse	TGAGCTCATTGAATGCTTGG	
IL-2-forward	GCAGGCCACAGAATTGAAAG	207 bp
IL-2-reverse	TCCACCACAGTTGCTGACTC	
IL-12-forward	CCTGCATCTAGAGGCTGTCC	243 bp
IL-12-reverse	CATCTTCTTCAGGCGTGTCA	
IL-6-forward	TTCCATCCAGTTGCCTTCTT	199 bp
IL-6-reverse	CAGAATTGCCATTGCACAAC	
IL-10-forward	CCAAGCCTTATCGGAAATGA	162 bp
IL-10-reverse	TTTTCACAGGGGAGAAAATCG	
TGF-b-forward	TGCGCTTGCAGAGATTAAAA	197 bp
TGF-b-reverse	GCTGAATCGAAAGCCCTGTA	
VEGFR2-forward	ACAGACAGTGGGATGGTCC	271 bp
VEGFR2-reverse	AAACAGGAGGTGAGCGCAG	
VEGFR1-forward	CCAACTACCTCAAGAGCAAAC	315 bp
VEGFR1-reverse	CCAGGTCCCGATGAATGCAC	
Arg1-forward	AAGAAAAGGCCGATTCACCT	201 bp
Arg1-reverse	CACCTCCTCTGCTGTCTTCC	
Perforin-forward	GATGTGAACCCTAGGCCAGA	161 bp
Perforin-reverse	GGTTTTTGTACCAGGCGAAA	
Granzyme B-forward	TCGACCCTACATGGCCTTAC	198 bp
Granzyme B-reverse	TGGGGAATGCATTTTACCAT	

were then maintained in RPMI complete medium for 48 hrs. Supernatants were analyzed for extracellular release of IFNγ by ELISA (using kit, OptEIA™, BD Pharmingen) following the manufacturer's protocol. (3-(4,5-dimethylthiazol-2-yl)-2,5-diphenyltetrazolium bromide (MTT) colorimetric assay was used to assess T-cell proliferation after exposure to TME [9].

Isolation of RNA and RT-PCR analysis

Total RNA was isolated from solid tumors (single-cell suspensions were obtained by enzymatic digestion) or purified cell populations from solid tumors. RNA was prepared using the Tri-reagent and cDNA synthesis was carried out using cDNA Synthesis Kit following the manufacturer's protocol and PCR were carried out using gene-specific primers. The oligonucleotide primers used are listed in Table 1 and Table 2. PCR products were identified by image analysis software for gel documentation (Gel Doc™ XR+ system, Bio-Rad, USA) following electrophoresis on 2% agarose gels stained with ethidium bromide.

Table 2
Primer sequences of various chemokine genes studied.

Name	Primer sequences (5′-3′)	Product size
CXCR3-forward	GCTGCTGTCCAGTGGGTTTT	67 bp
CXCR3-reverse	AGTTGATGTTGAACAAGGCGC	
CXCL9-forward	TGGGCATCATCTTCCTGGAG	204 bp
CXCL9-reverse	CCGGATCTAGGCAGGTTTGA	
CXCL10-forward	CCAAGTGCTGCCGTCATTTT	177 bp
CXCL10-reverse	CTCAACACGTGGGCAGGATA	
CCR5-forward	ACTGCTGCCTAAACCCTGTCA	78 bp
CCR5-reverse	GTTTTCGGAAGAACACTGAGAGATAA	
CCL3-forward	CCTCTGTCACCTGCTCAACA	163 bp
CCL3-reverse	GATGAATTGGCGTGGAATCT	
CCL4-forward	GCTGTGGTATTCCTGACCAAA	196 bp
CCL4-reverse	AAATCTGAACGTGAGGAGCAA	
CCL5-forward	CCCTCACCATCATCCTCACT	186 bp
CCL5-reverse	TCCTTCGAGTGACAAACACG	
CCL8-forward	ACGCTAGCCTTCACTCCAA	231 bp
CCL8-reverse	TCTGGAAAACCACAGCTTCC	
CXCR4-forward	TCAGTGGCTGACCTCCTCTT	203 bp
CXCR4-reverse	CTTGGCCTCTGACTGTTGGT	
CXCL12-forward	CTGCATCAGTGACGGTAAACC	142 bp
CXCL12-reverse	CAGCCGTGCAACAATCTGAAG	

Western blot analysis

The tumor tissue lysate or cellular lysate (50 μg) were separated on 6–20% SDS–polyacrylamide gel and transferred onto a polyvinylidene fluoride (PVDF) membrane (Millipore, USA) using the Bio-Rad Gel Transfer system. Immunoreactive proteins were detected by addition of the HRP color development reagent according to manufacturer's protocol.

Flow cytometric analysis of immune cellular markers

Flow cytometric analysis for surface phenotypic markers for T-cells, MDSCs and Tregs was performed after labeling with different anti-mouse fluorescence labeled antibodies (1 μl antibody for 1×10^6 cells) (CD8, CD4, CD25, CD11b, perforin, granzyme B, CD69, Gr1 and FasR) for 30 min as per manufacturer's recommendation. Cytometry was performed by FACS Caliber flow cytometer (Becton Dickinson, Mountainview, CA) and data was analyzed by Cell Quest (Becton Dickinson, Mountainview, CA) and FlowJo (Tree Star Inc., Ashland, USA) software. Percentage of each positive population and mean fluorescence intensity (MFI) were determined by using region statistics.

In vitro cytotoxicity with TME educated CD8⁺T-cells

Cytotoxicity of T-cells (primed with TME) against mouse B16 melanoma cells was tested by lactate dehydrogenase (LDH) release

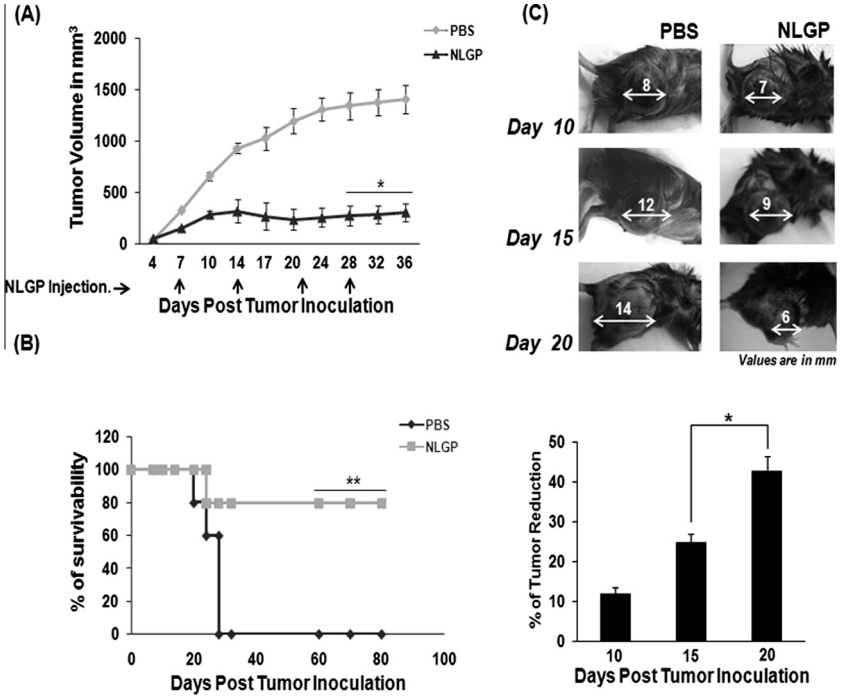

Fig. 1. C57BL6/J mice were inoculated with B16 melanoma F10 cells (2×10^5 cells/mice). After formation of palpable tumor, mice of experimental group ($n = 12$) was treated with NLGP (25 μg) s.c. once a week for 4 weeks in total and mice of control group ($n = 12$) received PBS only. Tumor (in mm^3) growth of mice of each group is presented till day 36 after the initiation of therapy (A) and their mean survival (B) are presented. Arrows indicate the time points of NLGP injections. Photographs of tumors from representative mice of each group at three different days (day 10, 15 and 20) are shown. Percent of tumor reduction in NLGP treated mice in comparison to PBS controls is presented.

assay using a cytotoxicity detection kit. In brief, 1×10^4 B16 melanoma cells were plated as target in 96-well cell culture plates. TME exposed $CD8^+$T-cells were added in triplicate as effector cells (Effector:Target; 10:1) in each well and incubated overnight. Cell-free supernatants were used to measure the level of released LDH using the formula:

$$\%\text{Cytotoxicity} = (\text{Lysis from Effector} + \text{Target Mixture} - \text{Lysis from Effector only}) - \text{Spontaneous Lysis/Maximum Lysis} - \text{Spontaneous Lysis} \times 100.$$

Statistical analysis

All results represent the average of five separate *in vitro* and three *in vivo* experiments. The number of experiments is mentioned in the results section and legends to figures. In each experiment, a value represents the mean of three individual observations and is presented as mean ± standard deviation (SD). Statistical significance was established by unpaired *t*-test using INSTAT 3 Software.

Results

NLGP therapy restricts B16 melanoma growth in C57BL/6 mice

Mice with established B16 melanoma growth on around 7th day of tumor inoculation were either PBS treated or administered with NLGP (25 μg/mice) weekly for 4 weeks in total. Result of such treatment schedule on melanoma bearing mice is presented in Fig. 1A–C, and indicates significant protection. This result shows progression of the disease in 13/20 (65%) NLGP treated mice, in comparison to 19/20 (95%) mice in control group. Moreover, tumor volume in NLGP treated mice with progressive disease is significantly less than controls (Fig. 1a, b). Again, number of tumor free animals is more in the mice group that received NLGP (7/20 (35%)) than in the group that received PBS only (1/20 (5%)) by 60 days post-tumor inoculation. Survival benefit of NLGP treated mice is 95% (19/20) on day 60 vs 5% (1/20) in PBS group ($p < 0.001$) (Fig. 1c).

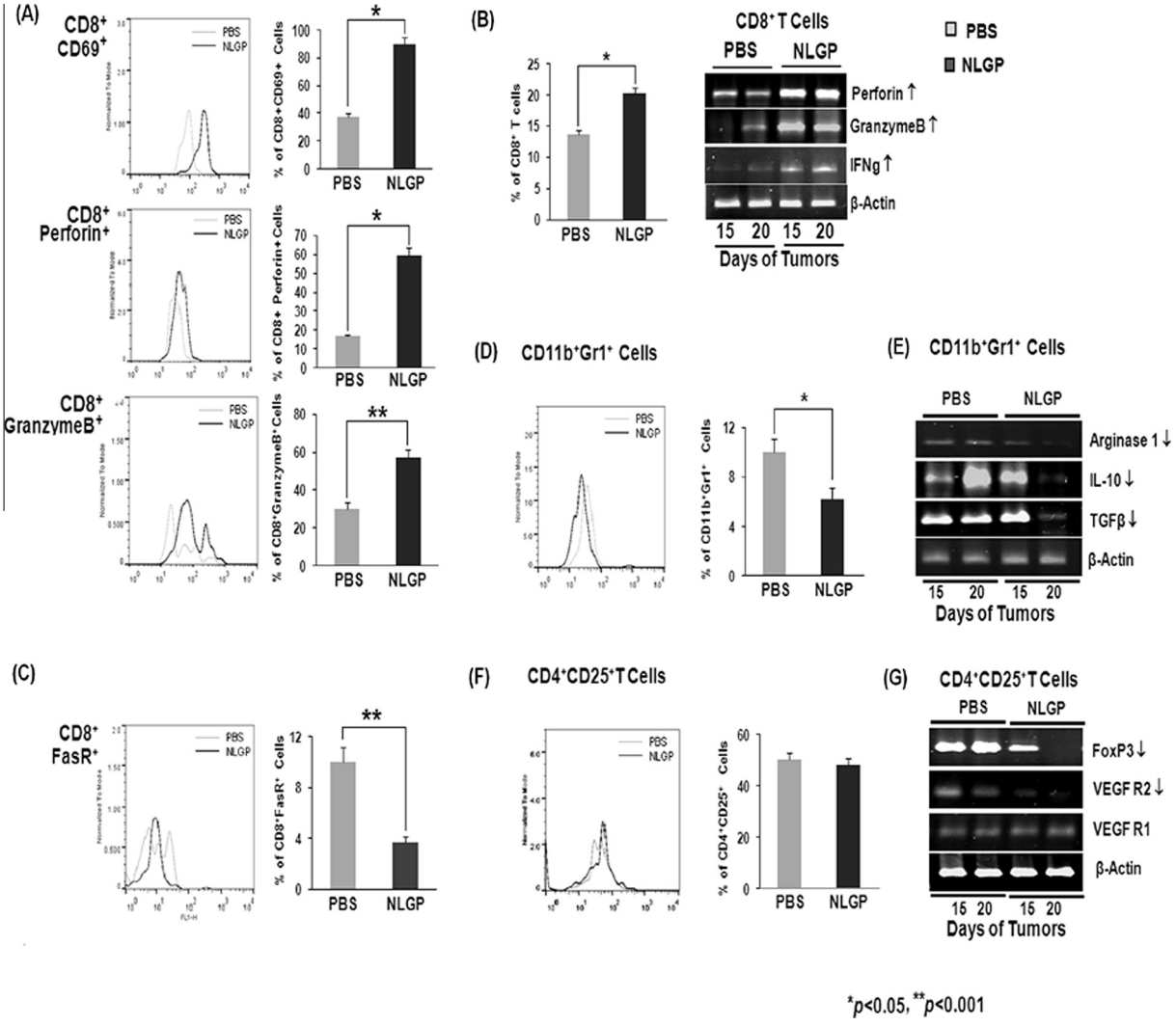

Fig. 2. Single cell suspension was prepared from tumors (day 20) of PBS and NLGP treated mice. (A) Proportion of activated T cells were measured by double labeling of $CD8^+$ cells with CD69, perforin, granzymeB antibodies and analyzed by flow cytometry after gating $CD8^+$T cells. (B) $CD8^+$T cells were purified from tumors and transcriptional profiling of various genes was studied by RT-PCR. (C) Cells were stained together with FasR and CD8 antibodies and percent of $FasR^+$ cells within $CD8^+$T cell population were measured by flow cytometry. (D) Cells were stained with CD11b and Gr1 antibodies and percentage of $Gr1^+$ cells were measured within $CD11b^+$ population, all FACS analysis were performed using Flowjo software, $^*p < 0.05$, $^{**}p < 0.001$. (E) $Gr1^+$ cells were purified from tumors by MACS and expressions of Arg1, IL-10 and TGF-β were studied by RT-PCR. (F) Cell suspensions were labeled together with CD4 and CD25 and percentage of $CD25^+$ cells was shown within $CD4^+$ T cell population, as assessed by flow cytometry. (G) $CD4^+CD25^+$ cells were purified from tumors by MACS and expressions of Foxp3, VEGFR1 and VEGFR2 were studied by RT-PCR.

NLGP optimizes the level of effector and regulatory cells within TME

As we reported previously that NLGP can't kill tumor cells directly [14] and modulates immune system [15,20], next we attempted to understand the immune mechanism of NLGP mediated restriction of B16 melanoma growth by studying effector and regulatory immune cells within TME. A considerable activation of $CD8^{+}$T cells was observed within NLGP-TME in comparison to PBS-TME, as represented by higher expression of CD69. These cells also expressed a greater proportion of IFNγ, perforin and

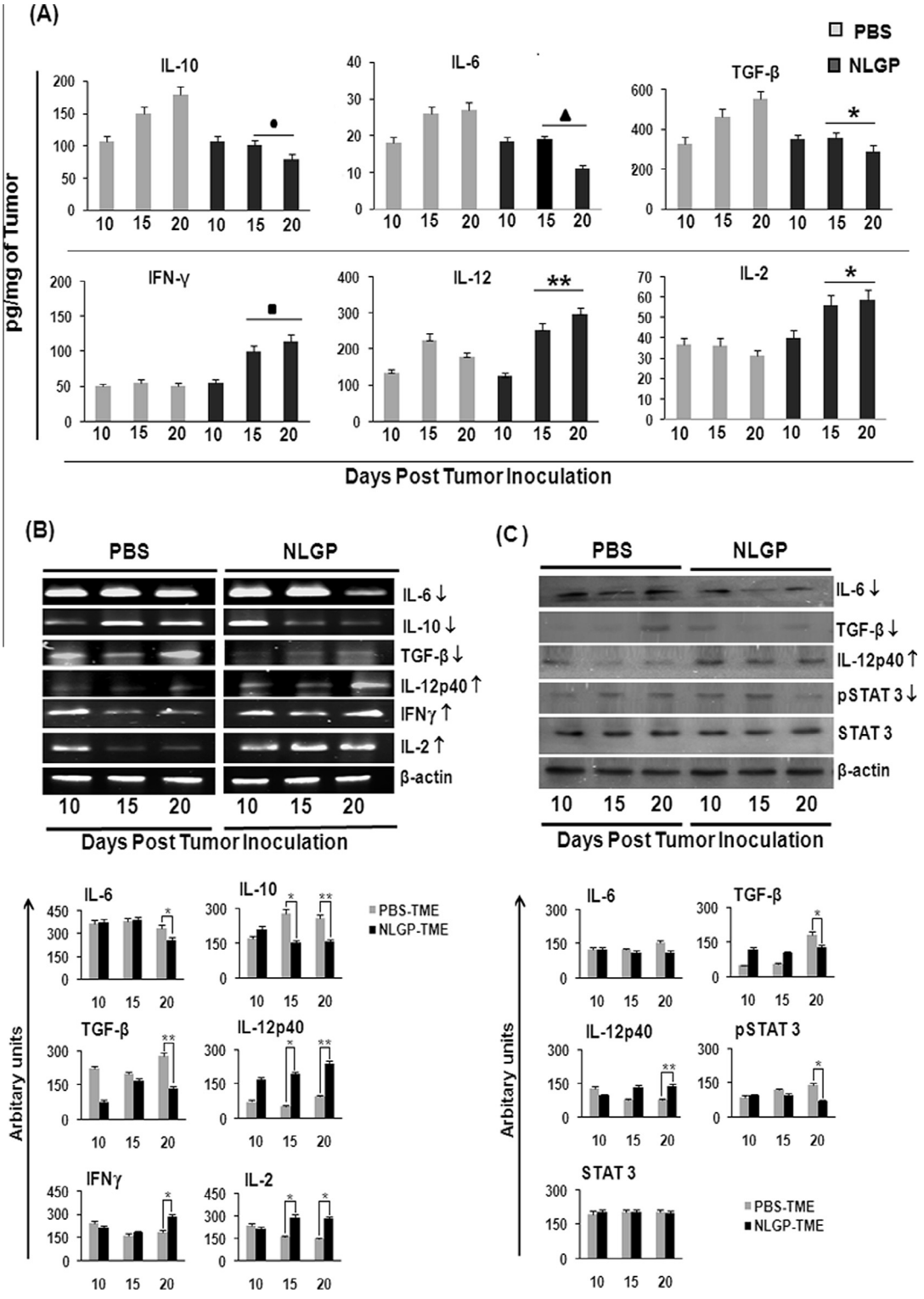

Fig. 3. NLGP modulates immunosuppressive cytokine milieu within TME. (A) Tumor tissues (100 mg) were harvested from B16Melanoma bearing C57BL6/J mice and lysed by freeze-thaw technique in PBS supplemented with a cocktail of protease inhibitors. Tumor tissue lysates, representing TME from either PBS or NLGP treated mice ($n = 6$ in each case) were assessed for IL-10, IL-6, TGFβ, IFNγ, IL-12, and IL-2 by ELISA in three different time points and quantitated as pg/mg of tumor tissues ± SE. $^{*}p = 0.01$, •$p = 0.02$, ▲$p = 0.005$, $^{**}p = 0.001$, ■$p = 0.03$, in comparison to PBS treated. (B) Total RNA was isolated from tumors of PBS and NLGP treated mice ($n = 4$, in each case) to analyze genes of IFNγ, IL-2, IL-12, IL-6 and IL-10 by RT-PCR. (C) IL-6, TGFβ, IL-12, STAT3 and *p*STAT3 levels were studied in total protein isolated from tumors of PBS and NLGP treated mice ($n = 4$, in each case) by Western blot analysis. Bar diagrams indicates quantitative expressions depicted in the RT-PCR and western blot analysis.

granzymeB (all representative of an active effector status) evaluated by flow cytometry and RT-PCR (Fig. 2A and B). We also found a much reduced FasR positivity within $CD8^+$T cells within NLGP-TME. This finding indicates that NLGP might protect $CD8^+$T cells from activation induced cell death (AICD) and helps their better survival within TME (Fig. 2C).

At the same time, a much lower proportion of MDSCs were found in tumors from NLGP treated mice (Fig. 2D), however, no significant change was detected in case of regulatory T-cells (Fig. 2E). mRNAs were isolated from Purified MDSCs and Tregs from both PBS and NLGP TME were used to isolate mRNAs and subjected to transcriptional analysis for some functionally relevant genes for MDSCs and Tregs. In purified MDSCs from NLGP-TME, Arginase1, TGFβ and IL-10 were significantly downregulated (Fig. 2E). Inspite of decrease in number of Tregs in NLGP treated group, a prominent down-regulation of Foxp3 and VEGFR2 gene expression was noted without any change in VEGFR1 (Fig. 2F).

NLGP optimizes the level of type1 and regulatory cytokines within TME

Optimization of the cellular functions within TME of NLGP treated mice prompted us to evaluate the status of secretory cytokines and growth factors. Cellular stress, aberrant growth and death of cancer cells generate many tumor associated factors that can enhance type2 inflammatory responses that lead to tumor progression [21]. To elucidate cytokine and growth factor status within TME, tumor lysates from NLGP and PBS treated groups were analyzed at three different time points (after tumor inoculation) by ELISA and immunoblotting. Tumors of NLGP treated mice exhibited significant up-regulated level of IFNγ, IL-2 and IL-12 (Fig. 3B–C) in day dependent manner and reduced release of IL-6, IL-10 and TGFβ (Fig. 3A,C) within TME, in comparison to PBS treated controls. In accordance with our earlier observation on NLGP mediated down-regulation of phosphorylation of STAT3 [14], here, we observed day dependent down-regulation of the same within NLGP-TME (Fig. 3C).

NLGP potentiates the migration of $CXCR3^+$ leukocytes against chemokine gradients within TME

Expression status of chemokine receptors/ligands is extremely important for T-cell migration within TME [22]. Using RT-PCR we have studied the status of chemokine receptors (ccr5, cxcr3 and cxcr4) and ligands (ccl3, ccl4, ccl5, ccl8, cxcl9, cxcl10 and cxcl12) at transcriptional level within TME. Results suggested upregulation of chemokine receptors, cxcr3 and ccr5, in NLGP-TME (Fig. 4). Ligands for cxcr3 (cxcl9, cxcl10) and ccr5 (ccl3, ccl4, ccl5 and ccl8) were also upregulated within NLGP-TME to varied extent (Fig. 4A

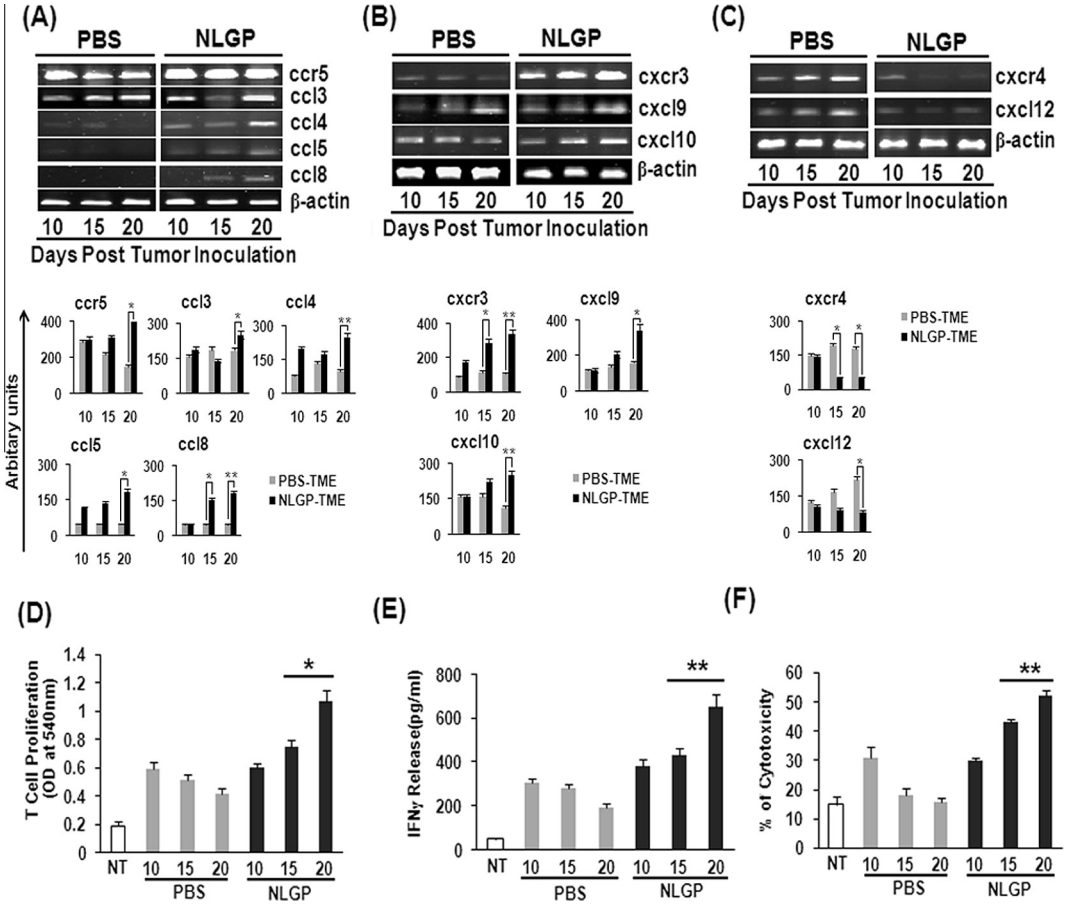

Fig. 4. NLGP normalizes chemokine network within TME and NLGP normalizes T cell functions within TME. Total RNA was isolated from tumors of PBS and NLGP treated mice. cDNA was prepared from RNA and RT-PCR was performed for different chemokine related genes, (A) ccr5, ccl3, ccl4, ccl5, ccl8; (B) cxcr3, cxcl9, cxcl10; (C) cxcr4, cxcl12. Bar diagrams indicates quantitative expressions depicted in the RT-PCR analysis. NLGP normalizes T cell functions within TME. Lysates were prepared from B16 melanoma tumors of different days, obtained from PBS and NLGP treated mice (PBS-TME and NLGP-TME). MNCs from normal C57BL6/J mice were incubated with PBS-TME and NLGP-TME for 120 hrs. (D) MNCs were then allowed to proliferate for 72 hrs and proliferation was determined by MTT assay. $^*p = 0.01$. (E) $CD8^+$T cells purified from TME exposed MNCs (by MACS) were further cultured for 48 hrs. Cell supernatants were used to measure IFNγ level by ELISA. $^{**}p = 0.001$. (F) Purified $CD8^+$T cells, as mentioned in E, were cultured with B16 melanoma cells to determine the tumor cell cytotoxicity by LDH release assay. $^{**}p < 0.001$. In every case, comparison was made between PBS-TME exposed T cells vs same exposed to NLGP-TME on day 15 and day 20.

and B). Downregulated expression of cxcr4 and cxcl12 in case of NLGP-TME than PBS controls indicated diminished regulatory cell (particularly MDSC) recruitment (Fig. 4C) at tumor site.

NLGP-TME educated CD8$^+$T-cells exhibit effector functions against melanoma cells

To further corroborate our *in vivo* results that normalization of TME by NLGP is directly associated with functional activation of CD8$^+$T-cells, we exposed mononuclear cells from naive mice for 120 hrs to TME (prepared from tumors of NLGP and PBS treated mice) and CD8$^+$T-cells were purified by MACS and analyzed subsequently. Functional analysis of such T-cells revealed that exposure of NLGP-TME helped them to proliferate more, release IFNγ in substantial quantity and lysed melanoma cells more conspicuously compared to PBS controls (Fig. 4D–F).

Discussion

Conventional therapies can reduce the tumor mass either by surgery, chemotherapy or by radiation mediated tumor killing [23,24]. Unfortunately, none is efficient for complete removal of tumor cells [25]. At the same time, these therapies promote immunosuppressive milieu by expansion of suppressor cells, paralysis of immune effector cells and creation of protumor cytokine-chemokine milieu within TME [26]). Such condition in TME further expands the residual tumor mass that often result in recurrence of the disease [27], by inducing active immune tolerance and escaping immune surveillance, thus fostering easy tumor cell proliferation, survival and migration [28].

In such view, present study demonstrated that therapeutic NLGP treatment subcutaneously once weekly for 4 weeks in total restricted melanoma growth and maintained 35% mice tumor free on day 60 post treatment, in comparison to 5% mice in PBS treated controls. Again, tumor growth rate of mice with progressed diseases was significantly less after NLGP treatment than similar mice with PBS injections. This observation is in parallel to our earlier report on sarcoma growth restriction by NLGP in Swiss mice [29]. As NLGP is neither a killer of cancer cells nor normal cells [14], the hypothesis is drawn on NLGP mediated immunomodulation. To confirm this hypothesis, we have sequentially analyzed different cellular and soluble mediators in tumor immune compartments from mice having PBS or NLGP treatment.

First attention was given on anti-tumor cytotoxic CD8$^+$T-cells [21]. Examination of such T cells from either PBS-TME or NLGP-TME revealed reversal of subdued T-cell activity due to NLGP treatment. In initial set of experiments, upregulation of CD8$^+$T-cells within NLGP-TME was observed and these cells have higher expression of activation marker CD69, along with cytotoxic molecules, perforin-granzyme B. In second set, normal T-cells were exposed to PBS-TME and NLGP-TME and NLGP-TME exposed T-cells function optimally, as examined by their proliferation, IFNγ secretion and tumor cell cytotoxicity. Furthermore, NLGP protects CD8$^+$T-cells from AICD. Thus, predominant effector cells can function optimally in NLGP influenced TME. In addition, immunosuppressive mechanisms operating in cancer patients significantly contribute to tumor progression and attenuate the efficacy of immunotherapies [30–32]. To elucidate the role of NLGP, we have examined the suppressor cells, MDSCs and Tregs and their functionally relevant molecules. Significant downregulation of MDSCs without any change in the level of Tregs was noted within TME. However, transcription factor required for Treg functionality, i.e., Foxp3, is decreased in NLGP-TME. MDSC derived cytokines, like, TGFβ, IL-10, were downregulated that may offer optimum environment for anti-tumor T-cell functions.

Effector and regulatory cells secrete various cytokines and chemokines depending on host tumor load. To find out these changes, tumors were harvested in day dependent manner from NLGP and PBS treated mice to look for Type1 and non-Type1 cytokine levels within TME. TME is generally non-type 1/regulatory cytokine dominated with greater content of IL-10, TGFβ and low IFNγ, IL-12 levels. We found that tumors of NLGP treated mice exhibited significant upregulated level of type1 cytokines (IL-2, IL-12 and IFNγ) (Fig. 3) in day dependent manner and reduced status of IL-6, IL-10 and TGFβ (type2 cytokines) (Fig. 3) within TME. This anti-tumor cytokine microenvironment helps in tumor eradication by several mechanisms. Although, these are yet to be identified, here, we have detected downregulation of phospho STAT3 in cells from NLGP-TME. STAT3 promotes the production of immunosuppressive factors (IL-6, IL-10 etc.) that phosphorylates STAT3 in diverse immune-cell subsets, altering gene-expression programs and, thereby, restraining anti-tumor immune responses leading to tumor-induced immunosuppression [33]. Simultaneously it is well documented that elevated levels of signaling components promote STAT3 phosphorylation in many tumor types and associated with a poor prognosis [34–36].

Chemokine-mediated T-cell migration is essential for optimal anti-tumor immune responses [22]. Resembling the cytokine network, chemokine milieu is also dysregulated within TME, thus, hampers homing of effector CD8$^+$T-cells in tumors. To ascertain chemokine receptor-ligand profile, we have analyzed cxcr3 and ccr5, and their corresponding ligands. It was found that ligands for ccr5 like ccl3, ccl4, ccl5 and ccl8 were increased within NLGP-TME. Same trends of up-regulation were observed in case of cxcl9, cxcl10, ligands for cxcr3. We also observed a marked down-regulation of cxcr4 and cxcl12 in NLGP treated tumors. *In vitro* studies suggested earlier that NLGP is efficient to correct cxcr3 and ccr5 dependent migration of lymphocytes and monocytes in HNSCC [15]. Obtained results suggest that chemokine gradients are normalized within NLGP-TME.

In conclusion, our data suggest that NLGP is efficient to diminish tumor growth by activating subdued T-cell functions within TME in co-operation with normalization of hyperactive suppressor cellular functions and maintaining optimum type-1/regulatory balance. NLGP may normalize pathological angiogenesis during regression of melanoma tumors as indicated by lowering of VEGF, VEGFR2 and HIF1α. Detail study in this field is awaiting.

Conflict of Interest

The authors have no conflict of interest.

Acknowledgements

We acknowledge Dr. Jaydip Biswas, Director, CNCI, India for providing necessary facilities. Thanks to Dr. Subrata Laskar, Burdwan University, India, for his help in characterization of NLGP. Thanks to Dr. Abhijit Rakshit for providing experimental animals. Partial financial support from Council of Scientific and Industrial Research, New Delhi (Grant No. 09/030/0063/2011EMR-I; 37(1524)/12/EMR-II) and from Indian Council of Medical Research, New Delhi (Grant No. 59/6/2011/BMS/TRM) is acknowledged.

References

[1] D. Berd, H.C. Maguire Jr., P. McCue, M.J. Mastrangelo, Treatment of metastatic melanoma with an autologous tumor-cell vaccine: clinical and immunologic results in 64 patients, J. Clin. Oncol. 8 (11) (1990) 1858–1867.
[2] G. Lizée, L.G. Radvanyi, W.W. Overwijk, P. Hwu, Immunosuppression in melanoma immunotherapy: potential opportunities for intervention, Clin. Cancer Res. 12 (7) (2006) 2359–2365.

[3] M.C. Schmid, J.A. Varner, Myeloid cells in the tumor microenvironment: modulation of tumor angiogenesis and tumor inflammation, J. Oncol. 2010 (2010) 1–10.
[4] S.A. Rosenberg, J.C. Yang, D.J. Schwartzentruber, P. Hwu, F.M. Marincola, S.L. Topalian, et al., Immunologic and therapeutic evaluation of a synthetic peptide vaccine for the treatment of patients with metastatic melanoma, Nat. Med. 4 (3) (1998) 321–327.
[5] T.L. Whiteside, Immune suppression in cancer: effects on immune cells, mechanisms and future therapeutic intervention, Semin. Cancer Biol. 16 (1) (2006) 3–15.
[6] J.F. Aldrich, D.B. Lowe, M.H. Shearer, R.E. Winn, C.A. Jumper, R.C. Kennedy, Vaccines and immunotherapeutics for the treatment of malignant disease, Clin. Dev. Immunol. 2010 (2010) 697158.
[7] R. Baral, U. Chattopadhyay, Neem *(Azadirachta indica)* leaf mediated immune activation causes prophylactic growth inhibition of murine Ehrlich carcinoma and B16 melanoma, Int. Immunopharmacol. 4 (3) (2004) 355–366.
[8] R. Baral, I. Mandal, U. Chattopadhyay, Immunostimulatory neem leaf preparation acts as an adjuvant to enhance the efficacy of poorly immunogenic B16 melanoma surface antigen vaccine, Int. Immunopharmacol. 5 (7–8) (2005) 1343–1352.
[9] S. Goswami, A. Bose, K. Sarkar, S. Roy, T. Chakraborty, R. Baral, Neem leaf glycoprotein matures myeloid derived dendritic cells and optimizes anti-tumor T cell functions, Vaccine 28 (5) (2010) 1241–1252.
[10] K. Sarkar, A. Bose, K. Chakraborty, E. Haque, D. Ghosh, S. Goswami, et al., Neem leaf glycoprotein helps to generate carcinoembryonic antigen specific anti-tumor immune responses utilizing macrophage-mediated antigen presentation, Vaccine 26 (34) (2008) 4352–4362.
[11] A. Bose, K. Chakraborty, K. Sarkar, S. Goswami, T. Chakraborty, S. Pal, Neem leaf glycoprotein induces perforin-mediated tumor cell killing by T and NK cells through differential regulation of IFNgamma signaling, J. Immunother. 32 (1) (2009) 42–53.
[12] K. Sarkar, S. Goswami, S. Roy, A. Mallick, K. Chakraborty, A. Bose, et al., Neem leaf glycoprotein enhances carcinoembryonic antigen presentation of dendritic cells to T and B cells for induction of antitumor immunity by allowing generation of immune effector/memory response, Int. Immunopharmacol. 10 (8) (2010) 865–887.
[13] E. Haque, R. Baral, Neem (*Azadirachta indica*) leaf preparation induces prophylactic growth inhibition of murine Ehrlich carcinoma in Swiss and C57BL/6 mice by activation of NK cells and NK-T cells, Immunobiology 211 (9) (2006) 721–731.
[14] T. Chakraborty, A. Bose, S. Barik, K.K. Goswami, S. Banerjee, S. Goswami, et al., Neem leaf glycoprotein inhibits CD4+CD25+Foxp3+ Tregs to restrict murine tumor growth, Immunotherapy 3 (8) (2011) 949–969.
[15] K. Chakraborty, A. Bose, T. Chakraborty, K. Sarkar, S. Goswami, S. Pal, et al., Restoration of dysregulated CC chemokine signaling for monocyte/macrophage chemotaxis in head and neck squamous cell carcinoma patients by neem leaf glycoprotein maximizes tumor cell cytotoxicity, Cell. Mol. Immunol. 7 (5) (2010) 396–408.
[16] K. Chakraborty, A. Bose, S. Pal, K. Sarkar, S. Goswami, D. Ghosh, et al., Neem leaf glycoprotein restores the impaired chemotactic activity of peripheral blood mononuclear cells from head and neck squamous cell carcinoma patients by maintaining CXCR3/CXCL10 balance, Int. Immunopharmacol. 8 (2) (2008) 330–340.
[17] R. Yamanaka, T. Abe, N. Yajima, N. Tsuchiya, J. Homma, T. Kobayashi, et al., Vaccination of recurrent glioma patients with tumour lysate-pulsed dendritic cells elicits immune responses: results of a clinical phase I/II trial, Br. J. Cancer 89 (7) (2003) 1172–1179.
[18] J. Yu, R. Tian, B. Xiu, J. Yan, R. Jia, L. Zhang, et al., Antitumor activity of T cells generated from lymph nodes draining the SEA-expressing murine B16 melanoma and secondarily activated with dendritic cells, Int. J. Biol. Sci. 5 (2) (2009) 135–146.
[19] J.L. Bailey, Miscellaneous analytical methods, in: J.L. Bailey (Ed.), Techniques in Protein Chemistry, Elsevier Science Publishing, New York, 1967, pp. 340–346.
[20] A. Bose, K. Chakraborty, K. Sarkar, S. Goswami, E. Haque, T. Chakraborty, et al., Neem leaf glycoprotein directs T-bet-associated type 1 immune commitment, Hum. Immunol. 70 (1) (2009) 6–15.
[21] B.F. Zamarron, W. Chen, Dual roles of immune cells and their factors in cancer development and progression, Int. J. Biol. Sci. 7 (5) (2011) 651–658.
[22] L.M. Ebert, P. Schaerli, B. Moser, Chemokine-mediated control of T cell traffic in lymphoid and peripheral tissues, Mol. Immunol. 42 (7) (2005) 799–809.
[23] J.Y. Wong, L.E. Williams, L.R. Hill, R.J. Paxton, B.G. Beatty, J.E. Shively, et al., The effects of tumor mass, tumor age, and external beam radiation on tumor-specific antibody uptake, Int. J. Radiat. Oncol. Biol. Phys. 16 (3) (1989) 715–720.
[24] M. Yamamoto, H. Iizuka, M. Matsuda, K. Nagahori, K. Miura, J. Itakura, The indications for tumor mass reduction surgery and subsequent multidisciplinary treatments in stage IV hepatocellular carcinoma, Surg. Today 23 (8) (1993) 675–681.
[25] L. Zitvogel, L. Apetoh, F. Ghiringhelli, G. Kroemer, Immunological aspects of cancer chemotherapy, Nat. Rev. Immunol. 8 (1) (2008) 59–73.
[26] H.A. Alshaker, K.Z. Matalka, IFN-γ, IL-17 and TGF-β involvement in shaping the tumor microenvironment: the significance of modulating such cytokines in treating malignant solid tumors, Cancer Cell Int. 11 (2011) 1–12.
[27] M.J. Reinhardt, K. Kubota, S. Yamada, R. Iwata, H. Yaegashi, Assessment of cancer recurrence in residual tumors after fractionated radiotherapy: a comparison of fluorodeoxyglucose, L-methionine and thymidine, J. Nucl. Med. 38 (2) (1997) 280–287.
[28] W. Zou, Immunosuppressive networks in the tumour environment and their therapeutic relevance, Nat. Rev. Cancer 5 (4) (2005) 263–274.
[29] A. Mallick, S. Barik, K.K. Goswami, S. Banerjee, S. Ghosh, K. Sarkar, et al., Neem leaf glycoprotein activates CD8+T cells to promote therapeutic anti-tumor immunity inhibiting the growth of mouse sarcoma, PLoS One 8 (2013) e47434.
[30] C. Botti, E. Seregni, L. Ferrari, A. Martinetti, E. Bombardieri, Immunosuppressive factors: role in cancer development and progression, Int. J. Biol. Markers 13 (2) (1998) 51–69.
[31] W. Zou, T. Regulatory, Cells, tumour immunity and immunotherapy, Nat. Rev. Immunol. 6 (2006) 295–307.
[32] S. Sakaguchi, K. Wing, Y. Onishi, P. Prieto-Martin, T. Yamaguchi, Regulatory T cells: how do they suppress immune responses?, Int Immunol. 21 (10) (2009) 1105–1111.
[33] H. Yu, M. Kortylewski, D. Pardoll, Crosstalk between cancer and immune cells: Role of STAT3 in the tumour microenvironment, Nat. Rev. Immunol. 7 (1) (2007) 41–51.
[34] R.J. Leeman, V.W. Lui, J.R. Grandis, STAT3 as a therapeutic target in head and neck cancer, Exp. Opt. Biol. Ther. 6 (3) (2006) 231–241.
[35] K.M. Quesnelle, A.L. Boehm, J.R. Grandis, STAT-mediated EGFR signaling in cancer, J. Cell. Biochem. 102 (2) (2007) 311–319.
[36] R. Baral, A. Bose, C. Ray, S. Paul, S. Pal, E. Haque, et al., Association of early phase of colorectal carcinogenesis with STAT3 activation and its relevance in apoptosis regulation, Exp. Mol. Pathol. 87 (1) (2009) 36–41.